Journal of Chromatography, 559 (1991) 163–181
Elsevier Science Publishers B.V., Amsterdam

CHROM. 23 458

Optimization and evaluation of the performance of arrangements for UV detection in high-resolution separations using fused-silica capillaries

G. J. M. BRUIN, G. STEGEMAN, A. C. VAN ASTEN, X. XU, J. C. KRAAK and H. POPPE*
Laboratory for Analytical Chemistry, Nieuwe Achtergracht 166, 1018 WV Amsterdam (Netherlands)

ABSTRACT

The evaluation of arrangements for UV measurements in fused-silica capillaries as applied in, *e.g.*, high-performance capillary electrophoresis, capillary liquid chromatography and hydrodynamic chromatography is described. The various designs are characterized with respect to sensitivity, noise, linearity, contribution to the peak width and sensitivity to refractive index effects. Some guidelines are formulated, based on theoretical and experimental observations, in order to maximize the performance. A cell with a focusing lens in front of the capillary resulted in a higher sensitivity and linear range than a cell with an adjustable aperture width. With the U-cell, having a design which is comparable to Z-shaped cells and having a longer longitudinal light path, a substantial increase in signal-to-noise ratio was achieved. Some applications of the UV cells are shown.

INTRODUCTION

Detectors for capillary electrophoresis and other miniaturized techniques have been given much attention in recent years as a direct consequence of the demand for sufficient sensitivity in high-resolution separation techniques such as high-performance capillary electrophoresis (HPCE) [1], capillary liquid chromatography [2,3] and hydrodynamic chromatography (HDC) in packed columns [4] or open capillaries [5].

The most important requirements for designs of detection cell suitable for capillary separation methods are well known, *i.e.*, a small contribution to the peak width and a sufficiently low detection limit. UV detection has remained the most popular detection principle, although the sensitivity is low compared with other detection modes developed for capillary separation systems, such as electrochemical [6], mass spectrometric [7] and fluorimetric [8] detection. The latter methods are only available in research institutes so far.

In HPCE, UV detection is mostly applied in the "on-column" mode and the detection limits are in the 10^{-5}–10^{-6} mol l^{-1} range [9,10] as a result of the short available light path, the inside diameter of the capillary. In HPCE, this value usually does not exceed 100 μm. One of the first reports dealing with the evaluation of UV detectors was from Wahlbroehl and Jorgenson [9]. In their experimental set-up, the

0021-9673/91/$03.50

reference and sample light beams passed through 100-μm pinholes. They found concentration detection limits of $8.6 \cdot 10^{-7}$ mol l^{-1} for isoquinoline and $2.8 \cdot 10^{-7}$ mol l^{-1} for lysozyme. Further, an increase in noise was observed after applying a high voltage, probably caused by vibrations of the capillary. A UV cell with an adjustable aperture width was described by Wang *et al.* [10]. Determination of the linear range resulted in an upper limit of about $3 \cdot 10^{-3}$ mol l^{-1} and a concentration detection limit of $3 \cdot 10^{-5}$ mol l^{-1} for acetophenone in acetonitrile at 240 nm.

Grant and Steuer [11] presented a novel way to extend the path length for UV absorbance into the millimetre range by illuminating along the column axis. By adding a fluorescent marker to the background electrolyte, the indirect measurement of the incident light beam can be monitored a few millimetres from the outlet of the column.

Theoretical optimization of cell designs was done by Bruno *et al.* [12]. They used a three-dimensional ray tracing algorithm, which simulates the optical phenomena at the air–glass and glass–liquid interfaces. This enabled them to choose optical fibre dimensions for a given choice of capillary inside and outside diameters. The experimental use of optical fibres in capillary zone electrophoresis (CZE) with UV detection was also demonstrated by the same group [13] and by Foret *et al.* [14].

Chervet *et al.* [15] have shown the usefulness of a Z-shaped longitudinal capillary flow cell for capillary liquid chromatography (LC) and HPCE. The Z-cell is constructed as part of the capillary by bending a small section into a Z-shape. The path length of the cell is dependent on the length of the chosen template and that of the detector configuration. Recently, they demonstrated the use of this type of cell with a light path of 2–3 mm for the CZE separation of some nucleosides and peptides [16]. They found a sixfold improvement in signal-to-noise ratio and a loss in plate number ranging from 11 to 33% compared with on-column detection.

In this work, a comparison has been made between different UV flow cells for HPCE, *i.e.*, a cell with an adjustable aperture width, a cell with a focusing sapphire lens just in front of the capillary and a U-cell with a light path of 8 mm. Also, a comparison was made between two commercially available UV detectors with focusing lenses.

The following aspects of the performance of the cells were studied: sensitivity, upper limit of the linear range, concentration detection limit and linear range; sensitivity for refraction index changes; and contribution to peak broadening.

THEORY

UV absorption in cylindrical cells

The transmission of light through a cylindrical cell can be calculated as described by Hjertén [17] in 1967. He used the calculations to check the performance of UV detection in wide-bore capillaries (3 mm I.D., 7.8 mm O.D.). The following assumptions were made: no refraction and reflection of the light; monochromatic UV light; uniform intensity of the incident light beam; and 100% collection of transmitted light by the photocell.

Considering the Lambert–Beer law for every infinitely small liquid element (see Fig. 1) with path length $l (= 2\sqrt{r^2 - x^2})$ and integration of the intensity to x leads to the following expression for the transmission in the cell:

$$T = \frac{N}{N_0} = \frac{1}{2s} \int_{-s}^{s} \exp(-2\,\varepsilon'\,c\,\sqrt{r^2 - x^2})\,\mathrm{d}x \qquad (1)$$

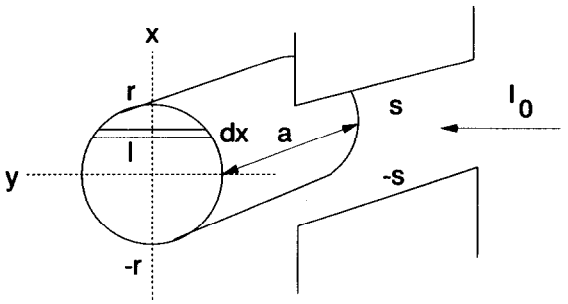

Fig. 1. Schematic representation of an on-column cell with adjustable aperture width. r = Radius of the capillary; s = half the aperture width.

where T is the transmission, N_0 is the number of photons per second that leave the cell in the case of no absorption, N is the number of photons when absorption takes place, r is the capillary radius, ε' is ln 10 times the molar absorptivity, s is half the slit width, c is the concentration and x is the position relative to the capillary centre. When $2\varepsilon' c \sqrt{r^2 - x^2} \ll 1$, eqn. 1 can be approximated as

$$T = \frac{1}{2s} \int_{-s}^{s} (1 - 2\,\varepsilon'\,c\,\sqrt{r^2 - x^2})\,dx \tag{2}$$

This integral can be found:

$$\begin{aligned} T &= 1 - \varepsilon'\,c \left[\sqrt{r^2 - s^2} + \frac{r^2}{s} \cdot \arcsin\left(\frac{s}{r}\right) \right] \\ &\approx \exp\left\{ -\varepsilon'\,c \left[\sqrt{r^2 - s^2} + \frac{r^2}{s} \cdot \arcsin\left(\frac{s}{r}\right) \right] \right\} \end{aligned} \tag{3}$$

Eqn. 3 is a good approximation when the absorbance is <0.1. In that case, the effective absorbance, being equal to $-\log T$, can be written as

$$A = \varepsilon\,c \left[\sqrt{r^2 - s^2} + \frac{r^2}{s} \cdot \arcsin\left(\frac{s}{r}\right) \right] \tag{4}$$

When the aperture width is adjusted to the inside diameter of the capillary ($s = r$), the effective light path is

$$l_{\text{eff}} = \frac{1}{2}\,\pi\,r \tag{5}$$

For absorbances >0.1, eqn. 1 cannot be rewritten as eqn. 2, but the integral can be obtained numerically using a computer program, such as Mathcad (version 2.5; Mathsoft). An example of this exercise is shown in Fig. 2. The theoretical calibration graphs for uracil (ε = 6980 l mol^{-1} cm^{-1}, λ = 234 nm) in a 50 μm I.D. capillary are

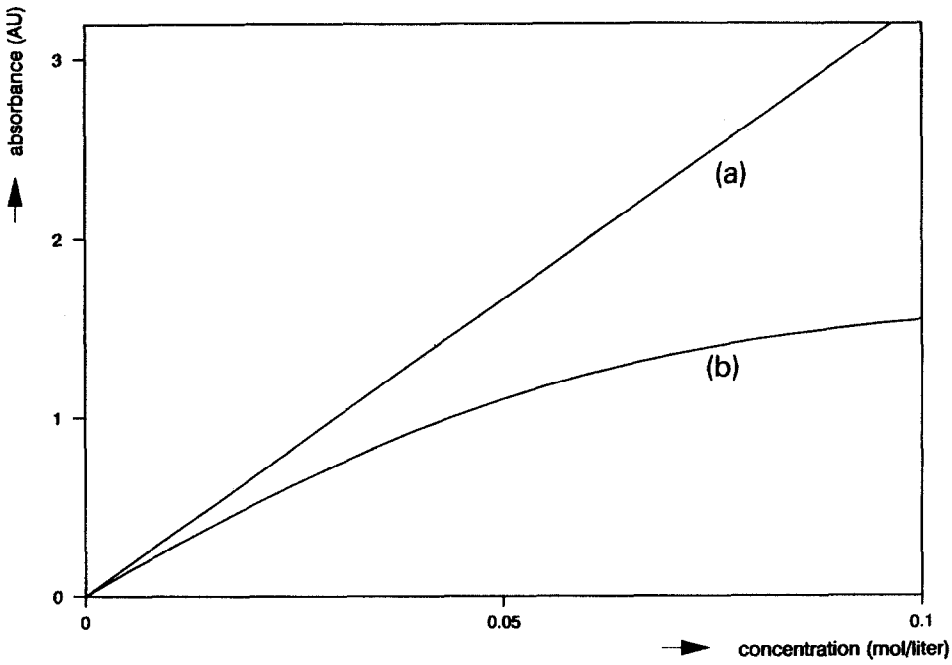

Fig. 2. Theoretical calibration graphs at different aperture widths. Capillary I.D., 50 μm. ε (uracil, 254 nm) = 6980 l mol^{-1} cm^{-1}. (a) Aperture width = 25 μm; (b) aperture width = 50 μm.

plotted against the concentration for two aperture widths, (a) 25 and (b) 50 μm. For an aperture width of 25 μm the sensitivity is higher as a result of the longer effective light path compared with an aperture width of 50 μm. The linearity of the calibration graph is also better because the shape of the cell approximates a rectangle. Further analysis of these results indicates that eqn. 2 can be used instead of eqn. 1 for absorbances <0.3.

When the aperture width has a value between the outside and inside diameters of the capillary, a fraction of the incident light beam does not take part in the absorption process at all. This light also reaches the photocell and degrades the sensitivity. Now, the total number of photons reaching the photocell per second can be expressed as

$$N = I_0\, a \int_{-r}^{r} \exp(-2\,\varepsilon'\, c\, \sqrt{r^2 - x^2})\, dx + 2\, I_0\, a \int_{r}^{s} dx \tag{6}$$

The transmission T can be written as

$$T = \frac{N}{N_0} = \frac{s - r}{s} + \frac{1}{2s} \int_{-r}^{r} \exp(-2\,\varepsilon'\, c\, \sqrt{r^2 - x^2})\, dx \tag{7}$$

In Fig. 3 the theoretical absorbance as a function of the aperture width is given. An increase in the absorbance with decreasing aperture width can be observed. At a width larger than the inside diameter of the capillary, the increase can be explained by

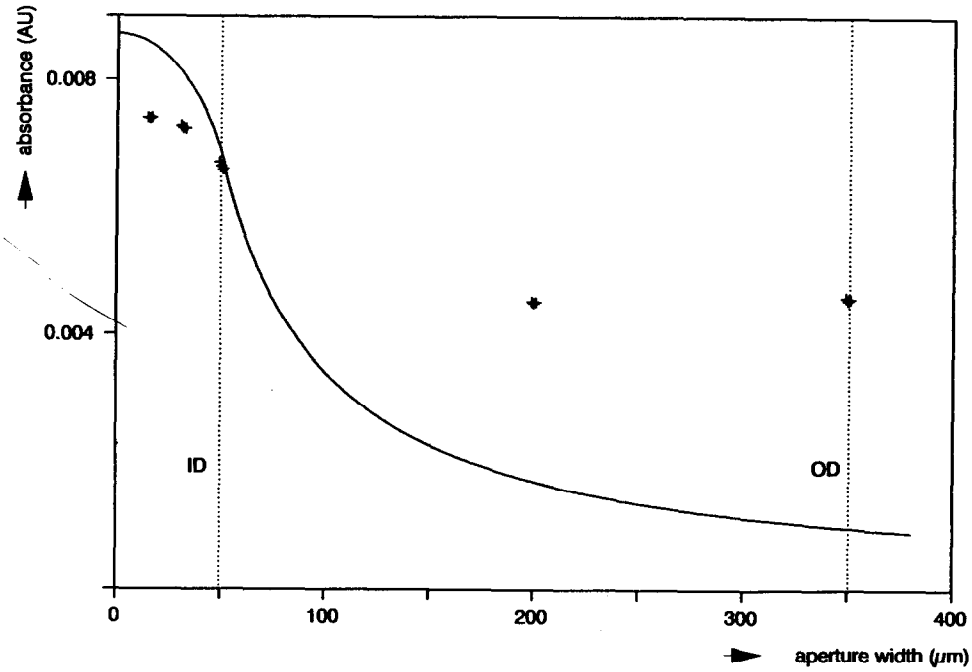

Fig. 3. Measured absorbance at various aperture widths (+) compared with the theoretical values (solid line). Capillary: 50 μm I.D., 350 μm O.D. Uracil concentration = $2.5 \cdot 10^{-4}$ *M*.

the fact that a larger fraction of the light is affected by the absorption process. The experimental values (+) will be discussed later.

Calculation of fraction of light that passes the detection window

Eqn. 7 can be rewritten as

$$T = \alpha + (1 - \alpha)\frac{1}{2r}\int_{-r}^{r} \exp(-2\,\varepsilon'\,c\,\sqrt{r^2 - x^2})\,dx \tag{8}$$

where α is the fraction of light that does not strike the liquid. α can be written as

$$\alpha = \frac{2s - 2r}{2s} \tag{9}$$

For small absorbances (*e.g.*, <0.3), this can be simplified to

$$T = \alpha + (1 - \alpha)T^* \tag{10}$$

where T^* is described by eqn. 3. Eqn. 10 would also be a good approximation for non-uniform light distributions.

We can express α as

$$\alpha = \frac{10^{-A} - 10^{-A^*}}{1 - 10^{-A^*}} \tag{11}$$

where A^* is the absorbance when all the light strikes the liquid and A the measured absorbance. If $10^{-A^*} \ll 10^{-A}$, or in other words when the absorbance of a compound is high, α can be calculated using

$$\alpha = 10^{-A} \tag{12}$$

This means that the value of α can be determined with a simple experiment.

Noise

For a good description of the performance of a detector, the signal-to-noise ratio is an important aspect to consider. Baumann [18] presented a theoretical treatment of signal, noise and signal-to-noise ratio for various types of detectors. He concluded that if the aperture width is decreased (or in other words the number of photons per second reaching the photocell becomes smaller), the relative noise level becomes higher as a result of shot noise.

Light refraction and reflection in cylindrical cells

In the theoretical treatment as described above, changes in the light intensity caused by reflection and refraction are neglected. Hjertén [17] pointed out that reflection losses are very small. Only at the outer edge of the capillary, where the angle of incidence is high, significant light reflection can occur.

Refraction can have a more significant impact. Light rays entering the detection window between the centre and the inside diameter of the capillary will not undergo much refraction. For light entering the capillary between the inside and outside diameters, the capillary glass wall works as a converging lens. Refraction and probably reflection can have a strong influence on the absorbance signal. To study these phenomena, a computer simulation can be a valuable tool. In the program developed in our laboratory, different parameters can be varied to optimize a certain cell configuration, *e.g.*, the distance from the focusing lens to the capillary, the inside and outside diameters of the capillary, the aperture width and the refraction index of the medium.

Some results of simulation are given in Fig. 4A–E for a cell with an adjustable aperture width and a cell with a focusing lens. It can be observed easily, on comparing Fig. 4A, B and C, that only at small aperture widths refraction and reflection can be neglected in the absorption calculations. This indicates that the assumptions made in the theoretical treatment of UV absorption in cylindrical cells are not always valid, *e.g.*, in the situation depicted in Fig. 4C.

When a sapphire lens is used to focus the light in the liquid flow, the performance of this type of cell depends strongly on the outside diameter of the capillary and the distance between the lens and the capillary (see Fig. 4D and E).

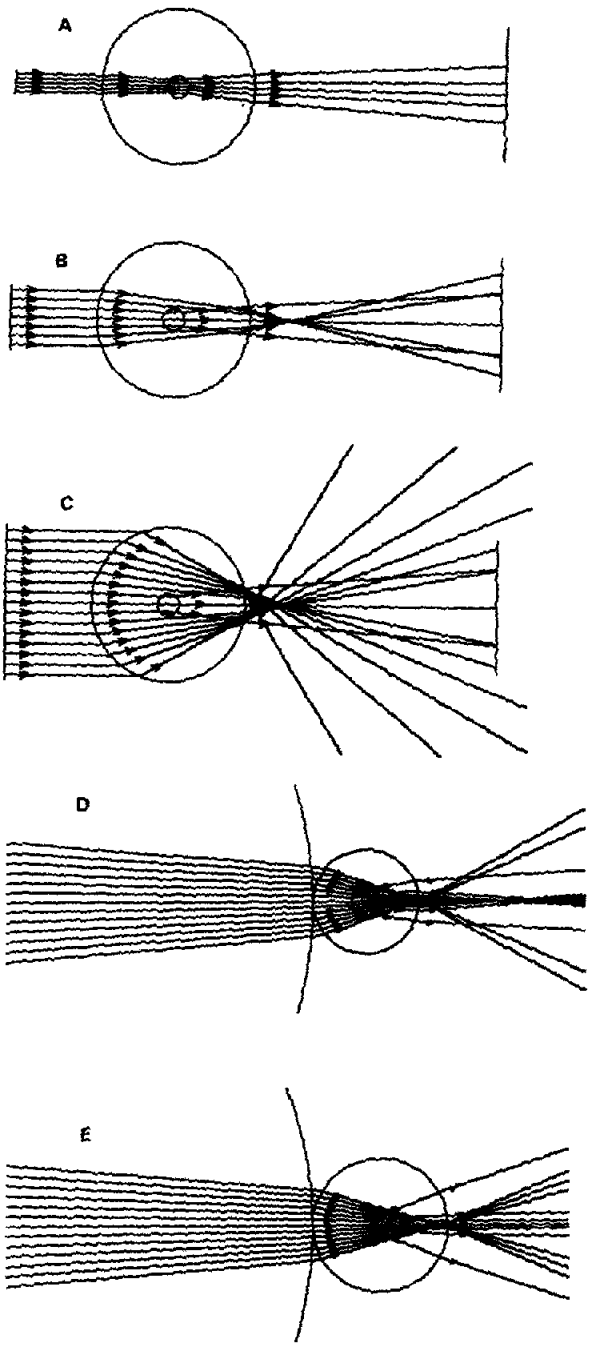

Fig. 4. Light refraction through cylindrical UV detection cells. Capillary: 50 μm I.D., 350 μm O.D. Cell A: (A) aperture width = 50 μm; (B) aperture width = 145 μm; (C) aperture width = 350 μm. Cell B: (D) capillary 75 μm I.D., 275 μm O.D.; (E) capillary 50 μm I.D., 350 μm O.D.

EXPERIMENTAL

Schematic diagrams of the four cells tested are depicted in Fig. 5A–D. Cell A is laboratory made and has an adjustable aperture width. The polyimide coating is burned off the capillary to provide an optical window by using an electrically heated wire. The window is cleaned with methanol. The capillary is fixed by sandwiching it between two pieces of metal covered with PTFE. One of the two metal pieces has a groove that retains the capillary in the correct position. Next, the body with the adjustable blades is placed on the connected metal pieces. The adjustment of the aperture width to the desired width can be performed by turning the small screws, which are connected with the blades. This has to be done while the entire cell is placed under a microscope. The length of the aperture along the capillary is 1 mm and the distance from the centre of the capillary to the photocell is 5 mm. The photocell itself has a square shape with an area of 36 mm^2.

Cell B is commercially available (Applied Biosystems, Foster City, CA, USA). It contains a focusing lens with a diameter of 2 mm, which is placed just in front of the optical window of the capillary (Fig. 5B).

Cell C closely resembles the design of cell B holder and is also commercially available (Linear Instruments, Reno, NV, USA). An advantage of this design is that the optical system (including the photocell) is placed outside the main cabinet of the detector, which facilitates thermostating the capillary over nearly the whole length (Fig. 5C).

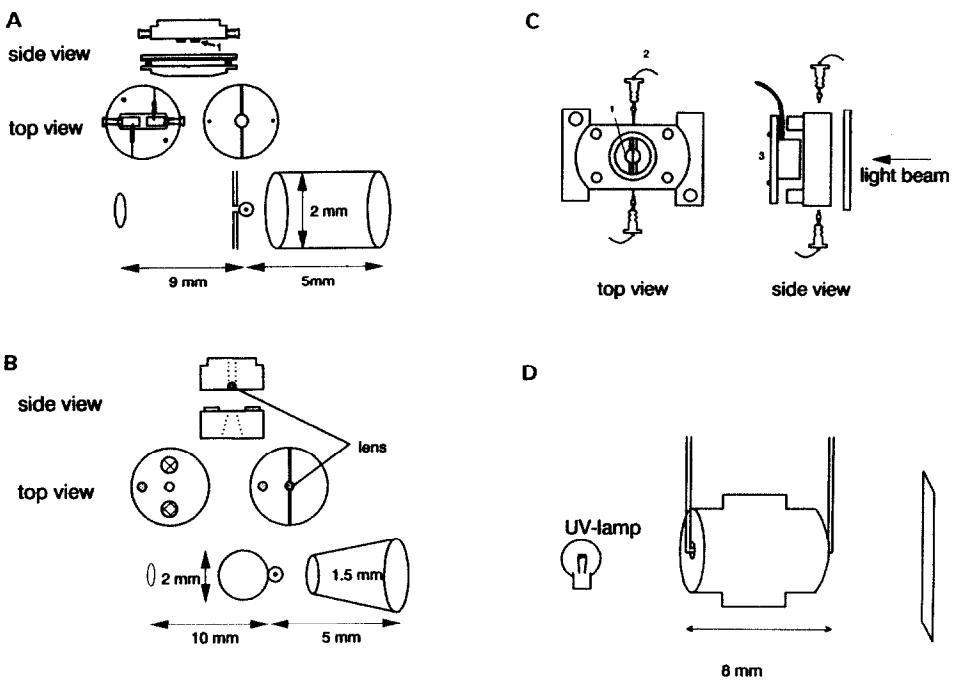

Fig. 5. (A) Scheme of cell A with adjustable aperture width (1). (B) Cell B with focusing lens. (C) Cell C with focusing lens. 1 = Lens; 2 = capillary; 3 = photocell. (D) Cell D (U-cell).

Cell D is the U-cell, custom-designed for use in a commercial detector (Applied Biosystems, Model 747) in cooperation with LC Packings (Amsterdam, Netherlands). It consists of a metal body with a hole along the central axis. The flow cell holder, which has the same outer dimensions as cell B, served as a template to align the capillary flow cell with the optical axis. The diameter of the hole matches the outside diameter of the inserted capillary, which is bent into a U-configuration. The bending of fused-silica tubing has been described elsewhere [19]. This design results in much longer path lengths, being 8 mm for the cells tested (Fig. 5D).

Two commercial UV detectors were used (Applied Biosystems, Model 757, and Linear Instruments, Model 203). The filter rise time of the UV detectors was 1 s in all the experiments.

All capillaries were supplied by Polymicro Technologies (Phoenix, AZ, USA). The calibration graphs for the different cell designs were constructed for uracil as test compound. Uracil was chosen because it has a broad absorption band in the vicinity of the wavelength chosen for the test (254 nm). The molar absorptivity was found to be 6980 l mol^{-1} cm^{-1}.

Calibration was carried out as follows. By injecting a large sample plug of known concentration (20–100 μl, depending on the inside diameter of the capillary), a constant signal is created for 2–3 min on the recorder. The plug is flushed through the capillary by using helium to pressurize a solvent reservoir filled with water.

The sensitivity S is defined as the ratio of the absorbance read out at the detector and the concentration. Noise is reported as peak-to-peak noise (four times the standard deviation of the noise, σ) over a period of 3 min. The concentration detection limit at the detector is defined as $c_{det} = 3\sigma/S$ (S = sensitivity).

The experimental set-up for the electrophoretic separations has been described in detail elsewhere [20]. When the influence of high voltage on the noise levels was studied, use was made of a phosphate buffer (0.05 M, pH 7.0).

Separation of oligonucleotide samples was performed in 100 μm I.D. gel-filled capillaries which were prepared according to the method described by Paulus and Ohms [21]. The temperature during the electrophoretic separations was kept at 25.0°C.

Cells B and D were applied for the separation of proteins in packed-column hydrodynamic chromatography (HDC). For this application, the fused-silica capillaries were directly coupled to the column outlet. The HDC column was a 150 × 4.6 mm I.D. stainless-steel column, filled with 1 μm non-porous silica particles. The particles were coated with polyethylene glycol (PEG 1000) according to Chang *et al.* [22].

Chemicals

Methanol (obtained from Merck, Darmstadt, Germany) was of high-performance liquid chromatographic grade. Methanol was checked for impurities by taking a UV spectrum of a 1% (v/v) solution in water. Oligodeoxyadenylic acid samples were purchased from Pharmacia (Woerden, Netherlands) and Isogen Biosciences (Amsterdam, Netherlands). Uracil, cytosine and thymine were supplied by Merck. Thyroglobulin (porcine) and albumin (chicken egg) were obtained from Sigma (St. Louis, MO, USA) and L-tyrosine from Merck.

RESULTS AND DISCUSSION

Cell with adjustable aperture width (cell A)

First, the results from cell A are discussed. The use of a fused-silica capillary of I.D. 50 μm and O.D. 350 μm resulted in calibration graphs as shown in Fig. 6. Each data point in the plot corresponds to the average of three measurements. Summarized data are given in Table I. It can be concluded from Fig. 6 and Table I that adjusting the slit width to the inside diameter results in the lowest concentration detection limit and the highest linear range. The higher sensitivity for a 20 μm aperture width is accompanied by higher noise. As predicted in the theoretical part, the highest sensitivity at the smallest aperture width is a result of the increased effective light path.

To obtain a better insight into these aperture width effects on sensitivity, the absorption at constant uracil concentration was measured at various aperture widths and compared with the theoretically predicted values, calculated from eqn. 7. The results are shown in Fig. 3. The value of the absorbance for an aperture width equal to the inside diameter is predicted with high accuracy. Also the trend towards higher absorbances at smaller aperture widths agrees with theory. However, at an aperture width larger than the inside diameter of the capillary, the recorded signal is much higher than theoretically expected. This deviation is caused by the assumption that refractive effects are negligible in the theoretical treatment used. This assumption cannot be justified, as can be seen in Fig. 4C. The fraction of light that enters the

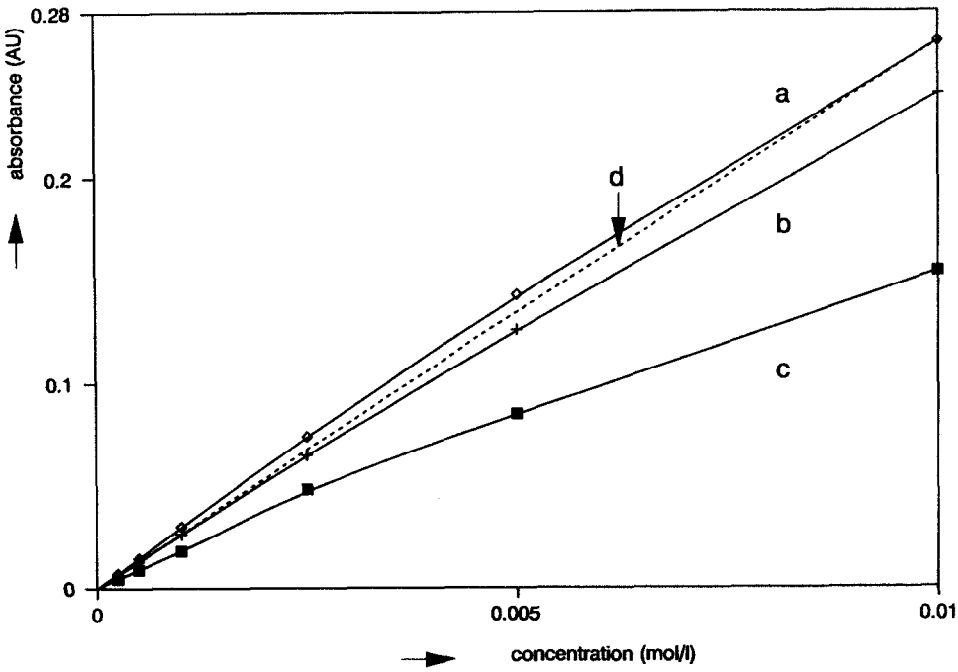

Fig. 6. Calibration graphs for cell A at various aperture widths. Capillary: 50 μm I.D., 350 μm O.D. Test compound: uracil. The data points are the average of three measurements. Aperture width: (a) 20; (b) 50; (c) 350 μm. The dashed line d represents the theoretical line for case b, calculated by using eqn. 4.

TABLE I

SENSITIVITY, NOISE, CONCENTRATION DETECTION LIMIT, UPPER LIMIT AND LINEAR RANGE AT THREE DIFFERENT APERTURE WIDTHS FOR CELL A

Aperture width (μm)	Sensitivity in linear range (absorbance l mol^{-1})	Peak-to-peak noise (absorbance)	c_{det} (l mol^{-1})	c_{upp} (l mol^{-1})	Linear range
20	29.5	$1.2 \cdot 10^{-4}$	$3.1 \cdot 10^{-6}$	$3.5 \cdot 10^{-3}$	1129
50	26.2	$5.0 \cdot 10^{-5}$	$1.4 \cdot 10^{-6}$	$3.5 \cdot 10^{-3}$	2500
350	18.6	$5.0 \cdot 10^{-5}$	$2.0 \cdot 10^{-6}$	$2.0 \cdot 10^{-4}$	100

capillary between the inside and outside diameter at the glass wall converges to the centre of the capillary. These refracted light rays partly do not reach the photocell, resulting in absorbance values higher than theoretically predicted. This also means that shielding these light rays with the adjustable aperture has no influence on the measured intensity, because they do not contribute to the intensity anyway. The absorbances for aperture widths smaller than the inside diameter are lower than theoretically predicted. This is probably caused by some experimental complications. Although it is not very difficult to adjust a certain aperture, it appears difficult to position the aperture completely symmetrically around the centre of the capillary. Slight misalignment can lead to significant deviations from the calculated effective light path.

A more detailed study on noise levels is shown in Fig. 7. In agreement with theory, there is an increase in the noise for a decreasing aperture width, no matter whether the capillary is installed or not. It can be seen that the noise is constant when the aperture is larger than the inside diameter with an installed capillary in the cell. This means that the intensity measured by the photocell is constant. It can be assumed, as discussed earlier, that a fraction of the incident light rays striking the optical window between the inside and outside diameters do not reach the photocell.

These experiments show that a decreased aperture width results in higher noise levels and higher sensitivities. There is an optimum aperture width where the highest signal-to-noise ratio can be found. As can be seen in Fig. 8, the highest signal-to-noise ratio and the resulting lowest concentration detection limit were found for an aperture width equal to the inside diameter of the capillary. This result has the additional advantage that adjustment of the aperture width to the inside diameter is easy to do, because the inner wall is clearly visible under the microscope.

A comparison between theoretical (line d) and experimental (line b) calibration graphs is given in Fig. 6 for a 50-μm aperture. The experimental data points for low concentrations agree very well with theory. There is a negative deviation from linearity at higher concentrations, starting at a lower concentration than theoretically expected. Accepting a 5% deviation, $3.5 \cdot 10^{-3}$ mol l^{-1} was found to be the upper limit. This value agrees well with upper limits from other test compounds and on-column cells as reported by others, *e.g.*, Wang *et al.* [10]. Theoretically, according to eqn. 7, a much larger upper limit, up to $2 \cdot 10^{-2}$ mol l^{-1}, is expected. It is difficult to find an explanation for this deviation.

The same calibration graph was obtained for a 75 μm I.D., 275 μm O.D.

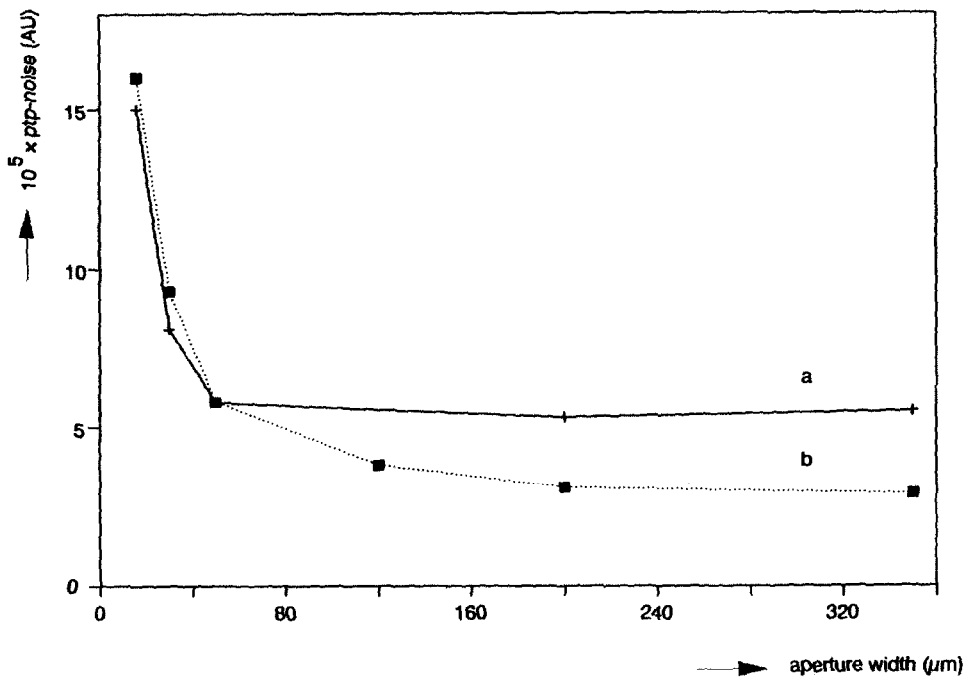

Fig. 7. Noise at various aperture widths, (a) with and (b) without an installed capillary (50 μm I.D., 350 μm O.D.) in the cell.

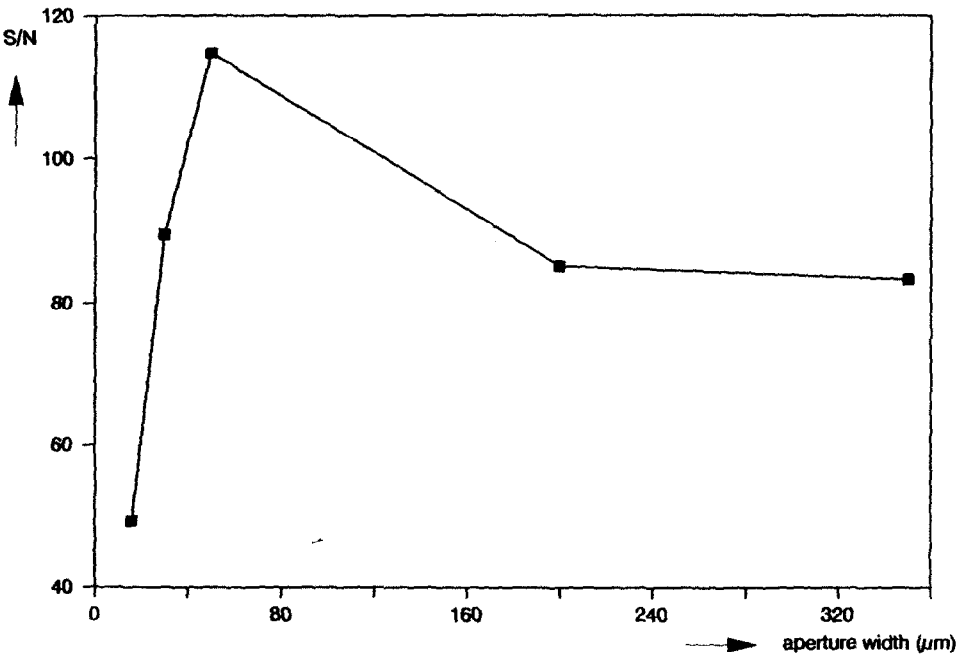

Fig. 8. Signal-to-noise ratio (S/N) at various aperture widths. Capillary: 50 μm I.D., 350 μm O.D. Compound: uracil, $c = 2.5 \cdot 10^{-4}$ mol l^{-1}.

capillary. This was done to make a fair comparison with the U-cell, which was supplied with a standard 75 μm I.D. capillary. The ratio of the sensitivities found for a 75 and a 50 μm I.D. capillary is 1.57, which agrees fairly well with the ratio of the inside diameters. The concentration detection limit and upper limit are $1.5 \cdot 10^{-6}$ and $2.5 \cdot 10^{-3}$ mol l^{-1}, respectively.

Wahlbroehl and Jorgenson [9] reported an increase in the noise when a high voltage was applied compared with the static measurements. This was possibly caused by vibrations of the capillary in the cell holder. In this work, no difference in noise level was found, which is an indication of good fixation of the capillary in the cell.

Cell with focusing lens (B)

The relevant results are summarized in Table II. Comparing the results for a 50 μm I.D. capillary with those obtained with cell A, it can be seen that the detection limits are nearly the same, whereas the linear range is nearly twice as large.

Changing the diameter from 50 to 75 μm results in a peculiar effect on the linear range, which becomes smaller, caused by the smaller upper limit. Apparently, the performance of this kind of cell depends strongly on the diameters of the capillaries used, as illustrated in Fig. 4D and E. Use of other than the optimum dimensions of the capillary will result in some misalignment. Also for this cell there was no increase in the noise levels when a high voltage was applied.

Cell with focusing lens (C)

Fig. 9 shows calibration graphs for four different inside diameters, from 25 to 100 μm I.D. Compared with cell B, the sensitivity is 2.5 and 2.0 times lower for a 50 and a 75 μm I.D. capillary, respectively, with cell C. Also, the noise is roughly five times lower than for cell B, which results in slightly improved detection limits for cell C. Because of the lower sensitivity and the non-linearity of the calibration graphs, it was suspected that in this device a substantial part of the light does not strike the liquid. The factor α describing this (see Theoretical) was determined by measuring the absorbance of a saturated solution ($c > 0.25\ M$) of potassium dichromate and using eqn. 12. The results are summarized in Table III. In Table III, also the calculated width of the light beam, $2s$, is given by substituting the α values for the four diameters in eqn. 9. The average light beam width is 139 μm. This means that capillaries having an I.D. $\gtrsim 140$ μm, should not give a sensitivity loss caused by by-passing effects.

TABLE II

SENSITIVITY, NOISE, CONCENTRATION DETECTION LIMIT AND UPPER LIMIT FOR CELL B

I.D. (μm)	Sensitivity in linear range (absorbance 1 mol^{-1})	Peak-to-peak noise (absorbance)	c_{det} (l mol^{-1})	c_{upp} (l mol^{-1})	Linear range
50	30.8	$5.5 \cdot 10^{-5}$	$1.3 \cdot 10^{-6}$	$5.8 \cdot 10^{-3}$	4142
75	48.5	$8.5 \cdot 10^{-5}$	$1.3 \cdot 10^{-6}$	$4.5 \cdot 10^{-3}$	3461

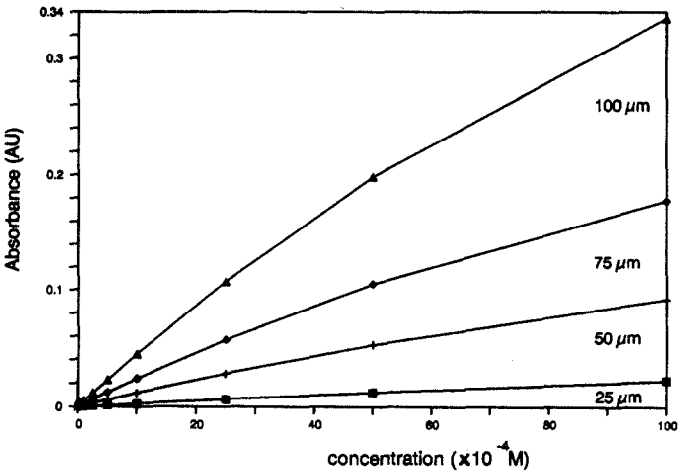

Fig. 9. Calibration graphs for cell C with four different I.D. capillaries (100, 75, 50 and 25 μm I.D.) as indicated. Test compound: uracil.

U-cell (D)

Two U-cells, made according to the same procedure [18], were evaluated and some of the results obtained are summarized in Table IV. The calibration graphs show strong non-linearity, which complicates the determination of the upper limit and the linear range. The sensitivities and the related concentration detection limits are rough estimates from measurements in the low concentration range. The non-linear character can be explained by complicated refraction and reflection patterns at the position where the light beam enters the capillary. Here the capillary is sharply bent, almost at right-angles. Although the non-linearity is a problem, it can be circumvented by calibration of the detection system.

The sensitivity of U-cells 1 and 2 is roughly 30 times higher than those found for cells A–C. It is remarkable that the two cells, although nominally the same, have different characteristics; cell 1 has a lower sensitivity and a lower noise level than cell 2, which results in comparably low detection limits ($9.8 \cdot 10^{-8}$ and $1.2 \cdot 10^{-7}$ mol l^{-1}, respectively). These detection limits are about fifteen times lower than those for cells A and B. On going to higher concentrations, the gain in signal-to-noise ratio decreases

TABLE III

CALCULATED α AND LIGHT BEAM WIDTH AT FOUR INNER DIAMETERS FOR CELL C

I.D. (μm)	A^* (absorbance)[a]	$A_{measured}$ (absorbance)	α	w_{beam} (μm)
25	2.7	0.08237	0.827	144
50	5.4	0.2072	0.620	131
75	8.1	0.3263	0.472	142
100	11	0.5512	0.281	139

[a] A^* is calculated using $A^* = \varepsilon cl$; $\varepsilon = 4037$ l mol^{-1} cm^{-1}.

TABLE IV

SENSITIVITY, NOISE AND CONCENTRATION DETECTION LIMIT FOR THE U-CELLS

Cell No.	Sensitivity in linear range (absorbance l mol^{-1})	Peak-to-peak noise (absorbance)	c_{det} (mol l^{-1})
1	950	$1.3 \cdot 10^{-4}$	$9.8 \cdot 10^{-8}$
2	1400	$2.2 \cdot 10^{-4}$	$1.2 \cdot 10^{-7}$

because of the non-linearity. This effect is clearly demonstrated in Fig. 10, where the signal-to-noise ratio for the three cell types is plotted against concentration.

Sensitivity for changes in the refractive index

A plug of a 1% (v/v) solution of methanol in water was injected to evaluate the response to a small change in refractive index of the streaming liquid flow. A plug of water was injected as a reference. As can be seen in Fig. 11A and B, the signal is nearly negligible for cell A and very small for cell B. Cell D is very sensitive to changes in the refractive index. The large signal as shown in Fig. 11C, injection 2, corresponds to a UV absorbance resulting from injection of $2 \cdot 10^{-6}$ *M* uracil.

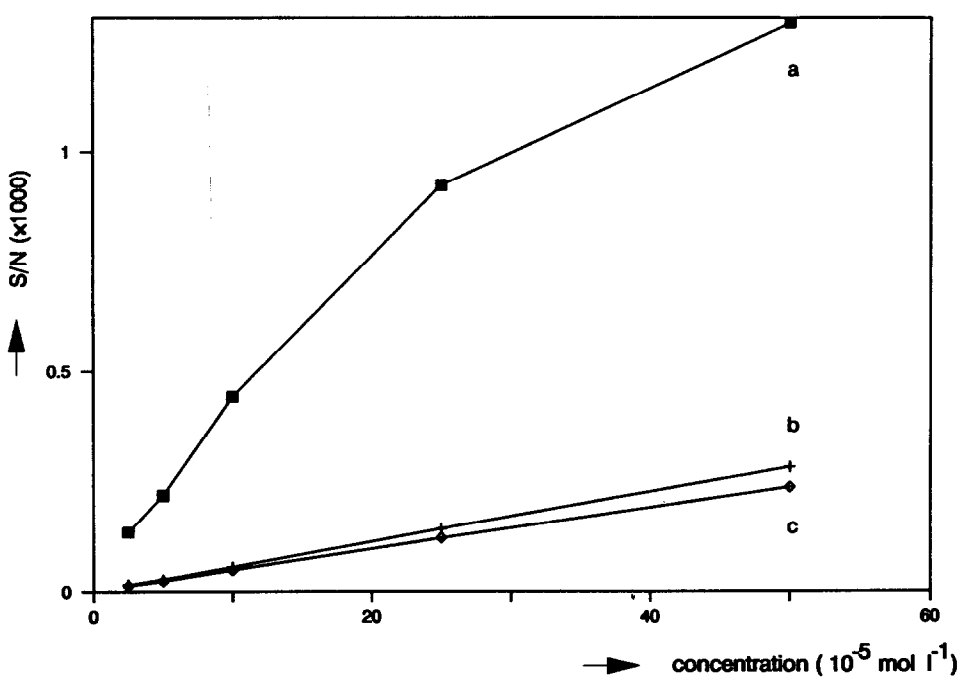

Fig. 10. Signal-to-noise ratio (S/N) for (a) cell D, (b) cell B and (c) cell A *versus* uracil concentration.

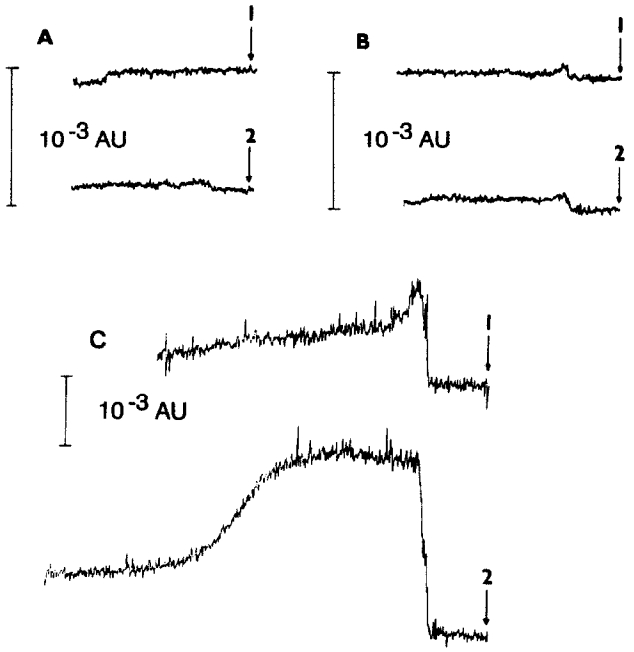

Fig. 11. Signal caused by changes in the refractive index after injection of 1% (v/v) aqueous methanol solution. Capillary: 75 μm I.D., 275 μm O.D. (A) Cell A; (B) cell B; (C) cell D; (1) injection of water and (2) injection of 1% (v/v) aqueous methanol in each instance. Arrows indicate injection points.

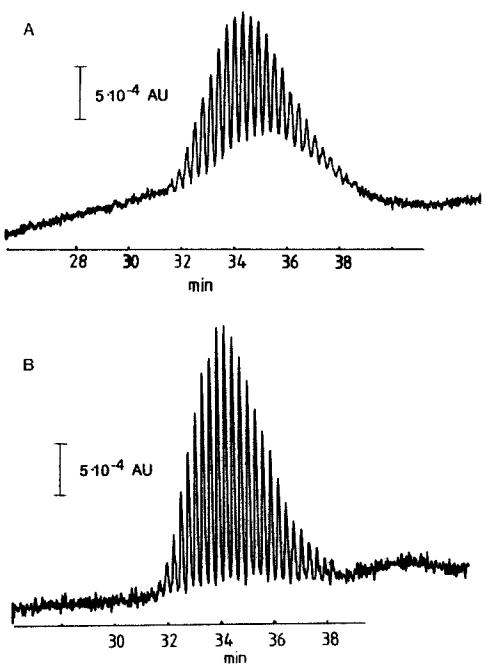

Fig. 12. CGE separation of a sample of oligonucleotides $p(dA)_{40-60}$. Buffer composition: 100 m*M* Tris, 100 m*M* boric acid, 2 m*M* EDTA, 7 *M* urea (pH 8.85). Capillary: 100 μm I.D., 220 μm O.D. Gel composition: 7.5% T, 3.3% C. UV detection at 260 nm. (A) Cell A; (B) cell B; aperture width 100 μm.

Contribution to peak width

This aspect will not be treated theoretically in detail here because it has been reported already by others [23,24]. Only some examples of efficient capillary electrophoretic and hydrodynamic chromatographic separations will be presented.

Fig. 12A and B show high-efficiency separations performed in gel-filled capillaries for a sample of oligonucleotides $pd(A)_{40-60}$ obtained with cells A and B, respectively. When cell B is used, all the peaks are baseline resolved. This good resolution is impaired when cell A is used. The influence of the detection cell length is very pronounced here. The length standard deviation of the separation (estimated from Fig. 12B, where external effects seem to be small) is 0.3 mm. The theoretical contribution to the peak width from a detection cell with an aperture length of 1.0 mm

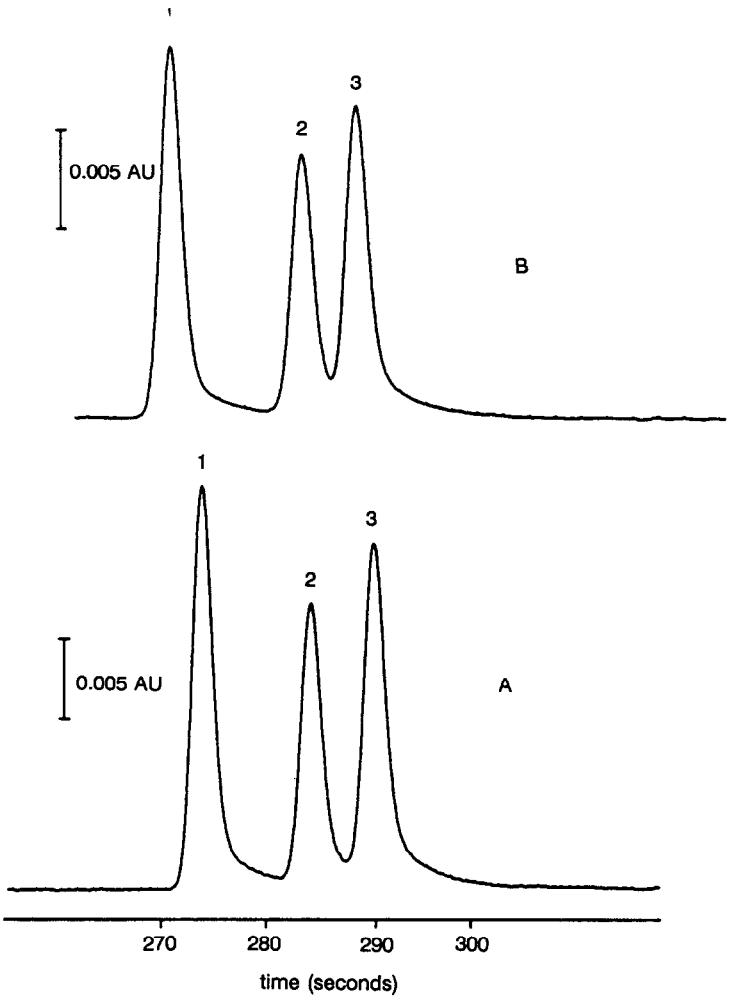

Fig. 13. MECC separation of (1) uracil, (2) cytosine and (3) thymine. Capillary: 50 μm I.D., 350 μm O.D. UV detection at 260 nm. (A) Cell A; (B) cell B.

along the capillary axis is $\sigma_{z,det} = 1.0/\sqrt{12} = 0.29$ mm. If a contribution of 5% from the detection cell to the total peak broadening is accepted, then it follows that

$$\sigma_{det} \leqslant 0.3\sigma_{sep} \tag{13}$$

A loss in resolution of about $\sqrt{2}$ can be expected in this particular separation. Hence, in case of capillary gel electrophoretic (CGE) separations, where plate numbers in the range of several millions can be achieved, it is preferable to use cells with a small aperture length along the capillary (< 100 μm).

Another comparison of this type, a micellar electrokinetic capillary chromatographic (MECC) separation of uracil, cytosine and thymine, is shown in Fig. 13A and B. There is a small decrease in efficiency of *ca.* 5% (from $N = 84\,000$ to 80 000 for peak 2) when cell A is used instead of cell B. The standard deviations in length units, $\sigma_{z,tot}$, are 1.26 and 1.23 mm for cells A and B, respectively. The theoretical contribution to the peak width from cell A, being 0.29 mm, is smaller than $0.3\sigma_{z,sep}$. This means that for this separation a cell with a length of 1 mm along the capillary is acceptable.

For the U-cell, the value of $\sigma_{z,det}$, calculated in the same way, is 2.3 mm. Although the U-cell has the highest sensitivity, its use in the above-mentioned separations was not considered. Unacceptable contributions to the peak width can be expected.

Full advantage of the high sensitivity of the U-cell can be achieved for less efficient separations or for separations on a larger volume scale. An example is given

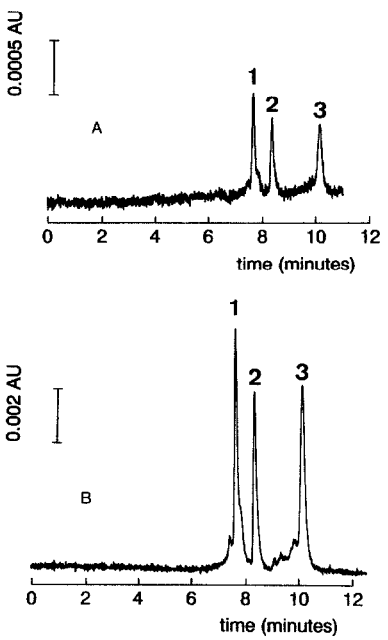

Fig. 14. HDC separation of some proteins. Mobile phase: 0.001 mol l^{-1} Tris–HNO_3 (pH 7.0) containing $5 \cdot 10^{-4}$ mol l^{-1} sodium azide. Wavelength, 230 nm; filter rise time, 0.2 s. (1) Thyroglobulin; (2) albumin; (3) L-tyrosine (1 mg ml^{-1} each). (A) Cell B; (B) cell D.

by packed column HDC. In earlier experiments with HDC [4,25] it was found necessary to perform detection in a fused-silica capillary fitted in the column outlet in order to avoid unacceptable peak broadening. This resulted in a serious loss of sensitivity. Cell D combines high sensitivity with acceptable peak broadening. HDC separations of proteins using cells B and D are shown in Fig. 14. The volume standard deviation of the separated compounds is so large ($\sigma_v \approx 5.5$ μl) that none of the cells contribute to the peak width. Cell D gives a much better detection limit. At the selected wavelength of 230 nm, it shows that cell D yields a four times better signal-to-noise ratio than cell B. However, this gain is smaller than the factor of *ca.* 20 reported at 254 nm and it decreases even further at lower wavelengths. This phenomenon can be explained by either mobile phase absorption at lower wavelengths or by the different refraction and reflection patterns at shorter wavelengths.

REFERENCES

1 J. W. Jorgenson and K. D. Lukacs, *Anal. Chem.*, 53 (1981) 1298.
2 J. Vindevogel, G. Schuddinck, C. Dewaele and M. Verzele, *J. High Resolut. Chromatogr. Chromatogr. Commun.*, 11 (1988) 317.
3 X. Xi and E. S. Yeung, *Anal. Chem.*, 62 (1990) 1580.
4 G. Stegeman, R. Oostervink, J. C. Kraak and H. Poppe, *J. Chromatogr.*, 506 (1990) 547.
5 R. Tijssen, J. P. A. Bleumer and M. E. van Kreveld, *J. Chromatogr.*, 260 (1983) 297.
6 R. A. Wallingford and A. G. Ewing, *Anal. Chem.*, 61 (1989) 98.
7 R. D. Smith, J. A. Loo, C. G. Edmonds, C. J. Barinaga and H. R. Udseth, *J. Chromatogr.*, 516 (1990) 157.
8 S. Wu and N. J. Dovichi, *J. Chromatogr.*, 480 (1989) 145.
9 Y. Wahlbroehl and J. W. Jorgenson, *J. Chromatogr.*, 315 (1984) 135.
10 T. Wang, R. H. Hartwick and P. B. Champlin, *J. Chromatogr.*, 462 (1989) 147.
11 I. H. Grant and W. Steuer, *J. Microcolumn Sep.*, 2 (1990) 74.
12 A. E. Bruno, E. Gassmann, N. Pericles and K. Anton, *Anal. Chem.*, 61 (1989) 876.
13 H. Lüdi, E. Gassmann, H. Grassenbach and W. Märki, *Anal. Chim. Acta*, 213 (1988) 215.
14 F. Foret, M. Deml, V. Kahle and P. Boček, *Electrophoresis*, 7 (1986) 430.
15 J. P. Chervet, M. Ursem, J. P. Salzmann and R. W. Vannoort, *J. High Resolut. Chromatogr.*, 12 (1989) 278.
16 J. P. Chervet, personal communication.
17 S. Hjertén, *Chromatogr. Rev.*, 9 (1967) 122.
18 W. Baumann, *Fresenius' Z. Anal. Chem.*, 284 (1977) 31.
19 J. P. Chervet, LC Packings, *Eur. Pat.*, No. 89106700, 1990.
20 G. J. M. Bruin, R. H. Huisden, J. C. Kraak and H. Poppe, *J. Chromatogr.*, 480 (1989) 339.
21 A. Paulus and J. I. Ohms, *J. Chromatogr.*, 507 (1990) 113.
22 J. P. Chang, Z. H. Rassi and Cs. Horváth, *J. Chromatogr.*, 319 (1985) 396.
23 K. Otsuka and S. Terabe, *J. Chromatogr.*, 480 (1989) 91.
24 X. Huang, W. F. Coleman and R. N. Zare, *J. Chromatogr.*, 480 (1989) 95.
25 J. C. Kraak, R. Oostervink, H. Poppe, H. Esser and K. K. Unger, *Chromatographia*, 27 (1989) 585.